

Long-range correlations and edge transport bifurcation in fusion plasmas

To cite this article: Y. Xu *et al* 2011 *Nucl. Fusion* **51** 063020

View the [article online](#) for updates and enhancements.

You may also like

- [A strategy to significantly improve the classification accuracy of LIBS data: application for the determination of heavy metals in *Tegillarca granosa*](#)
Yangli XU, , Liuwei MENG et al.
- [Negative correlation between frequency-magnitude power-law exponent and Hurst coefficient in the Long-Range Connective Sandpile model for earthquakes and for real seismicity](#)
Ya-Ting Lee, Luciano Telesca and Chien-chih Chen
- [On the interplay between turbulent forces and neoclassical particle losses in zonal flow dynamics](#)
R. Gerrú, S. Mulas, U. Losada et al.

Long-range correlations and edge transport bifurcation in fusion plasmas

Y. Xu¹, D. Carralero², C. Hidalgo², S. Jachmich¹, P. Manz^{3,4},
E. Martínez⁵, B. van Milligen², M.A. Pedrosa², M. Ramisch³,
I. Shesterikov¹, C. Silva⁶, M. Spolaore⁵, U. Stroth³ and
N. Vianello⁵

¹ Association 'Euratom-Belgian state', Ecole Royale Militaire - Koninklijke Militaire School, B-1000 Brussels, Belgium, on assignment at Plasmaphysik (IEK-4) Forschungszentrum Jülich, Germany

² Association EURATOM-CIEMAT, 28040 Madrid, Spain

³ Institut für Plasmaphysik, Universität Stuttgart, D-70569 Stuttgart, Germany

⁴ Center for Energy Research, University of California at San Diego, San Diego, CA 92093, USA

⁵ Consorzio RFX, Associazione Euratom-ENEA sulla Fusione, 35127 Padova, Italy

⁶ Associação Euratom/IST, Instituto de Plasmas e Fusão Nuclear, 1049-001 Lisboa, Portugal

Received 31 December 2010, accepted for publication 7 April 2011

Published 13 May 2011

Online at stacks.iop.org/NF/51/063020

Abstract

Recently, a European transport project has been carried out among several fusion devices for studying the possible link between the mean radial electric field (E_r), long-range correlation (LRC) and edge bifurcations in fusion plasmas. The main results reported in this paper include: (i) the discovery of low-frequency LRCs in potential fluctuations which are amplified during the development of edge mean E_r using electrode biasing and during the spontaneous development of edge sheared flows in stellarators and tokamaks. Evidence of nonlocal energy transfer and the geodesic acoustic mode modulation on local turbulent transport have also been observed. The observed LRCs are consistent with the theory of zonal flows described by a 'predator-prey' model. The results point to a significant link between the LRC and transport bifurcation. (ii) Comparative studies in tokamaks, stellarators and reversed field pinches have revealed significant differences in the level of the LRC. Whereas the LRCs are clearly observed in tokamaks and stellarators, no clear signature of LRCs was seen in the RFX-mod reversed field pinch experiments. These results suggest the possible influence of magnetic perturbations on the LRC, in agreement with recent observations in the resonant magnetic perturbation experiments at the TEXTOR tokamak. (iii) The degree of the LRCs is strongly reduced on approaching the plasma density-limit in tokamaks and stellarators, suggesting the possible role of collisionality or/and the impact of mean $E_r \times B$ flow shear on zonal flows.

(Some figures in this article are in colour only in the electronic version)

1. Introduction

Transport barriers are a crucial element for enhancing the confinement properties in magnetic confinement devices and therefore are of great importance for the development of magnetic fusion as an alternative energy source. Since the first discovery of H-mode and spontaneous transport barriers in the ASDEX tokamak [1], the reduction in turbulent transport by mean $E \times B$ sheared flows at the barrier location has been intensively investigated [2–5]. At present, there exists robust evidence on the importance of the radial electric field (E_r) to control edge plasma turbulence and hence for the development of edge plasma transport bifurcations. However, the mechanism governing the development of this bifurcation

is still one of the main scientific conundrums facing the magnetic fusion community.

In parallel, in recent years various experiments [6–9] have detected long-range correlations consistent with the theory of 'zonal flows' described by a predator-prey model, i.e. modes that are driven by zonal flow-turbulence interaction and with the potential to regulate turbulent transport [10, 11]. The coupling between fluctuations and flows is the basis for some bifurcation theory models of the L-H transition [12, 13]. Evidence of zonal flows linked to transport barriers has been reported in different fusion machines under different conditions [14, 15]. According to theory [10], the zonal flows are toroidally and poloidally symmetric potential structure ($m = n = 0$) with finite radial wavelength, a long distance

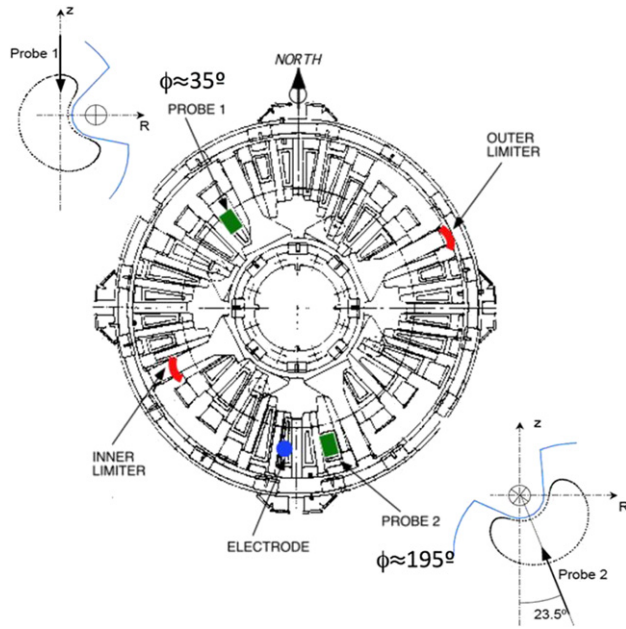


Figure 1. A schematic view of the top of the TJ-II stellarator showing an example for the measurement of LRCs of edge turbulence by two distant probe arrays.

cross-correlation of potential fluctuations along the same flux surface is naturally expected for zonal flows. Therefore, experimental exploration on the importance of LRCs of edge fluctuations for plasma confinement appears to be a paramount task.

In order to gain a further insight into the above issues, a European transport project has been recently executed among several machines for surveying the possible link between the mean $E_r \times B$ sheared flows, LRC and edge transport bifurcation in fusion plasmas. Common features have been shown on the results obtained in various devices, such as tokamaks, stellarators and reversed field pinch. In this article, we will present the experimental results measured in these different machines. The influence of the resonant magnetic perturbations (RMP) and plasma density on the LRC will also be reported.

The paper is organized as follows. In section 2 the experimental set-up among various devices is described. Section 3 presents the experimental results together with discussions and section 4 summarizes the conclusions.

2. Experimental set-up

The experiments were performed in several fusion devices for comparative studies. For measuring the LRC of edge fluctuations, multiple Langmuir probe arrays have been commonly used at the edge of these machines. As an example, the experimental set-up in the TJ-II stellarator is drawn in figure 1 to illustrate the detection of the LRCs. In the figure, one can see two probe arrays (probes 1 and 2) located at two different positions of the torus, separated about $\Delta\phi \approx 160^\circ$ toroidally and $\Delta\theta \approx 155^\circ$ poloidally [16]. The distance between these two arrays is more than 5 m. Both arrays were fast reciprocating and the probe tips were operated to detect the floating potential (V_{fl}) and ion saturation current

(I_s) fluctuations simultaneously at a sampling rate of 2 MHz. Similar probe settings were also made in other devices, as can be seen in the right column of table 1. The primary experimental conditions have been listed in table 1, where R and a denote the major and minor radii of the plasma, P_{ECRH} is the heating power on plasmas in the TJ-II [16] and TJ-K [18] stellarators, I_p is the plasma current in the TEXTOR [17] and ISTTOK [19] tokamaks as well as in the RFX-mod reversed field pinch device [20], B_T is the toroidal magnetic field and $\langle n_{e0} \rangle$ is the line-averaged density, respectively.

In the edge biasing experiments in TJ-II [16], TEXTOR [17], TJ-K [18] and ISTTOK [21], the biasing-induced improved confinement was realized using a biasing electrode inserted several cm inside the last closed flux surface (LCFS) and several hundred volts (see table 1) biased onto the limiter or vacuum vessel. In the TJ-II stellarator, a spontaneous L–H transition occurred with neutral beam injection (NBI) heating ($P_{NBI} \approx 450$ kW) on the ECRH target plasmas [22]. In all devices, the toroidal (or poloidal) LRCs between the fluctuation signals x and y , measured on the two distant probes, were estimated by computing their cross-correlation $C_{xy}(\tau) = \langle [x(t+\tau) - \bar{x}][y(t) - \bar{y}] \rangle / \sqrt{\langle [x(t) - \bar{x}]^2 \rangle \langle [y(t) - \bar{y}]^2 \rangle}$, where τ is the time lag.

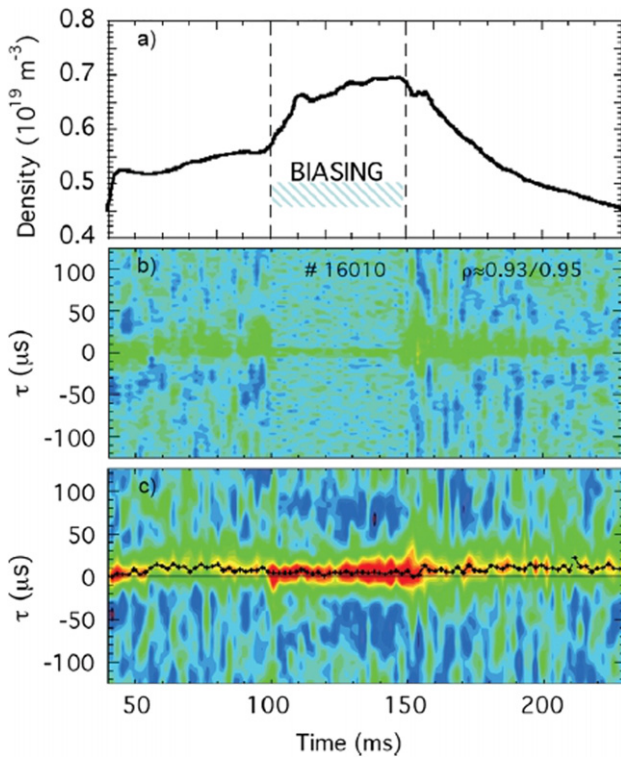
3. Experimental results and discussions

3.1. LRCs in electrode biasing and spontaneous H-mode experiments

Figure 2 plots the time evolution of the LRC of I_s and V_{fl} fluctuations measured by two toroidally/poloidally separated probes (radially around the same location inside the LCFS) during a biasing experiment in the TJ-II stellarator [16]. As shown in figure 2(a), the increase in the line-averaged density during the biasing phase indicates an improvement of particle confinement. From figure 2(b), one can see that both before and during biasing the LRC on the I_s signals is very small, revealing nearly no long distance cross-correlation on density fluctuations. In contrast, the LRC on V_{fl} fluctuations behaves very differently. Without biasing there exists a small cross-correlation on the V_{fl} signals while with biasing the LRC on V_{fl} fluctuations is substantially enhanced along with the occurrence of confinement improvement. It has been found that the amplified LRC on the V_{fl} signals during the biasing phase is dominated by low frequencies below 20 kHz and the phase delay between the two signals is close to zero (see also in figure 2(c)) [16], consistent with $n = 0$ mode structure for zonal flows. The results of the LRC on I_s and V_{fl} fluctuations measured by two toroidally spaced probe arrays (one is stationary and the other is fast reciprocating) at the TEXTOR tokamak [17] are depicted in figure 3(a), where the LRCs before and during the biasing phase are displayed in the left and right column, respectively. The top panels show the time traces of the fast probe moving from the scrape-off layer (SOL) into the edge region, whereas the stationary probe stays at a fixed radial position inside the LCFS. The results are very similar to those observed in the TJ-II stellarator, i.e. (i) in the discharge phase without biasing there is a small cross-correlation on the V_{fl} fluctuations when the two toroidally separated probes are localized around the same radial position

Table 1. Experimental conditions and main plasma parameters in various fusion devices for the measurements of LRCs under three different regimes: ohmic, electrode biasing and spontaneous L–H transition.

		R/a (m/m)	P_{ECRH} (kW)	I_p (kA)	B_T (T)	$\langle n_{e0} \rangle$ ($1 \times 10^{19} \text{ m}^{-3}$)	V_{bias} (V)	Distance of probe arrays (m)
Ohmic or electrode biasing	TJ-II stellarator	1.5/0.2	400		1	0.35 ~ 1.0	+300	5 $\Delta\phi \approx 160^\circ$, $\Delta\theta \approx 155^\circ$
	TEXTOR tokamak	1.75/0.48		200–250	1.9–2.25	1.0–3.0	+200–700	7 $\Delta\phi \approx 180^\circ$, $\Delta\theta \approx 0^\circ$
	TJ-K stellarator	0.6/0.1	1.8		0.072	0.01	+100	0.7 $\Delta\phi \approx 0^\circ$, $\Delta\theta \approx 180^\circ$
	ISTTOK tokamak	0.46/0.085		5–6	0.5	0.05–0.1	+100	1 $\Delta\phi \approx 120^\circ$, $\Delta\theta \approx 90^\circ$
	RFX-mod r.f. pinch	2.0/0.459		300	0.13	1.0		15 $\Delta\phi \approx 30^\circ$, $\Delta\theta \approx 0^\circ$
	Spontaneous L–H transition	TJ-II stellarator		400 450 (P_{NBI})			3.0	

**Figure 2.** Increase in the LRC on V_{fi} fluctuations during the biasing experiment in the TJ-II stellarator [16]. (a) Time trace of line-averaged density. Contour plot of cross-correlation in (b) I_s and (c) V_{fi} fluctuations as a function of time measured toroidally/poloidally apart by two probe arrays, which are located at about the same radial position ($r/a = 0.93$ and 0.95) in the plasma edge.

inside the LCFS ($r/a \approx 0.96$); (ii) during biasing the LRC in V_{fi} fluctuations strongly increases at those locations; (iii) both before and during biasing, no cross-correlation is seen in the I_s signals. Figure 3(b) plots the frequency spectrum of V_{fi} fluctuations measured by the fast probe at $r/a \approx 0.96$ before and during the biasing. With biasing, the fluctuation power at high frequencies (>4 kHz) is reduced, in agreement with the paradigm of $E \times B$ shear decorrelation on small-scale turbulence. However, at low frequencies (<3 kHz), the fluctuation power is strongly enhanced. Therefore, the large LRC appeared in the biasing phase is dominated by

low-frequency zonal flows [17]. Similar amplification of the LRC on V_{fi} signals has also been observed in the ISTTOK tokamak during the biasing-induced improved confinement, in which the LRC has been found to be associated with the geodesic acoustic mode (GAM) oscillations [21].

In the low temperature plasma regime at the TJ-K stellarator, the LRCs on V_{fi} and I_s (\propto density) fluctuations have been measured by poloidal multi-array probes, consisting of 128 pins on 4 adjacent flux surfaces [18]. Unlike in former devices, the results at TJ-K show the existence of the LRC on both potential and density fluctuations with a poloidal mode $m = 4$, as shown in the top figures in figure 4. With biasing, the LRCs are both amplified and the poloidal modes of the LRC in V_{fi} and I_s fluctuations change into $m = 0$ and 3, respectively (see bottom figures in figure 4).

In addition to biasing-induced improved confinement, an increase in the LRC has also been observed during a spontaneous L–H transition in the NBI-heated plasmas in the TJ-II stellarator [22]. Figure 5(a) plots the maximum value of the LRC on V_{fi} fluctuations as a function of the line-averaged density in NBI plasmas. As plasma density increases, ECRH-heated plasmas give way to pure NBI-heated plasmas, and a spontaneous L–H transition occurs at density $\approx 2 \times 10^{19} \text{ m}^{-3}$. At the same time, the cross-correlation reaches the highest value. This process can also be clearly seen in figure 5(b), where the time evolution of the LRC and $1/H_\alpha$ signal across the transition time is displayed. One can see that the LRC increases significantly at the bifurcation time when H_α drops abruptly. In all the above cases, the observed LRCs with toroidal mode $n \approx 0$ are dominated by low-frequency fluctuations, and hence, are consistent with zonal flows.

Moreover, evidence of nonlocal energy transfer between the drift-wave turbulence and zonal flows has been observed in the TJ-K stellarator, where the energetic interaction between ambient turbulence and zonal flows has been investigated in a 2D wave-number space (k_r and k_θ in radial and poloidal directions, respectively) using extensive poloidally spaced multi-array probes arranged on four neighboring flux surfaces [23]. The energy transfer was computed using the technique proposed by Camargo *et al* [24]. With the sum of all k_r contributions, the results for given $k_{\theta 1}$ and $k_{\theta 2}$ components are illustrated in figure 6. In the figure T_{tot}^V represents the total transfer function and the curve is a projection of the 2D data

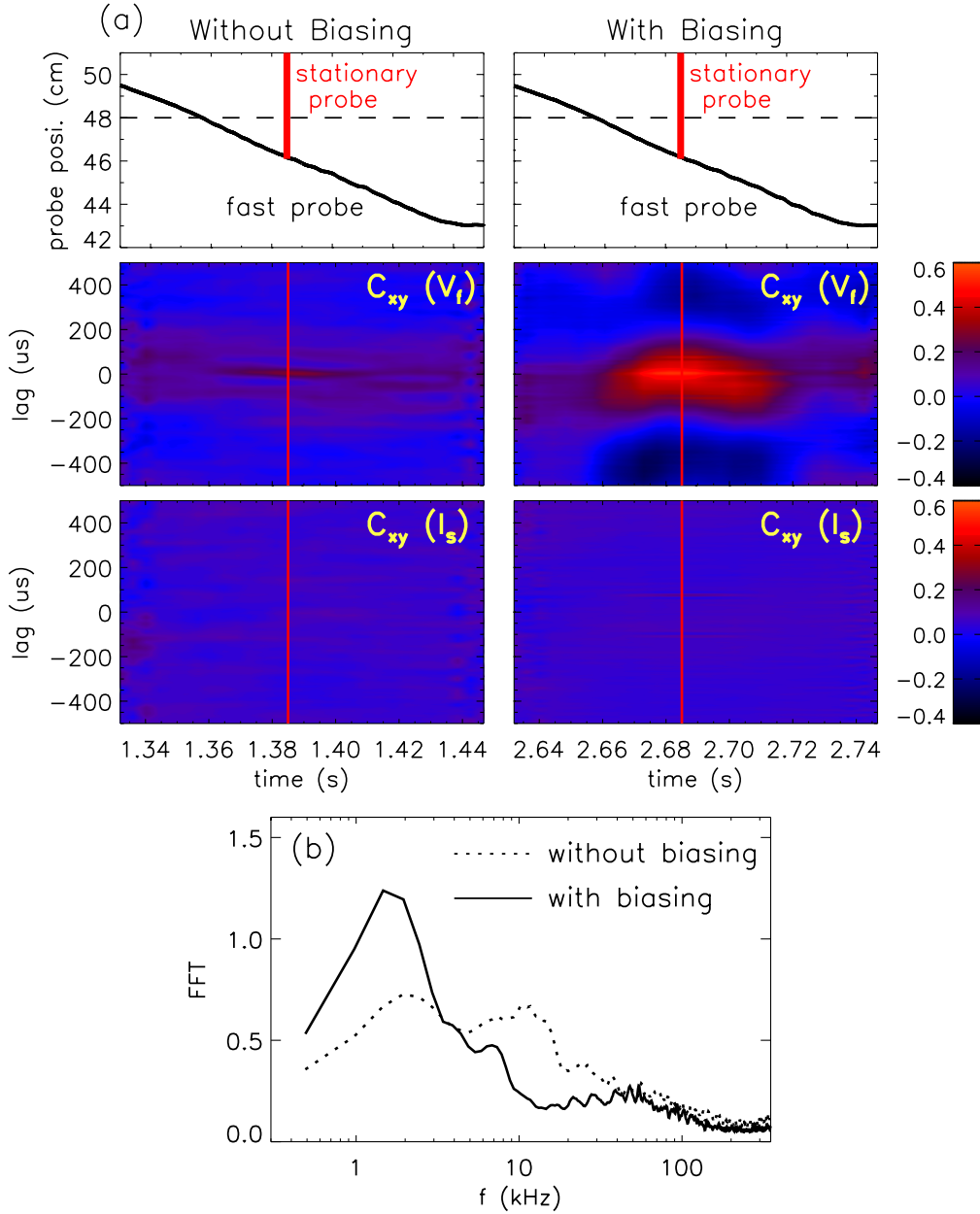


Figure 3. (a) Increase in the LRC on V_n fluctuations during the biasing experiment at the TEXTOR tokamak [17]. Time history of fast/stationary probes (top panels) and the contour plot of cross-correlation on V_n (middle panels) and I_s (bottom panels) fluctuations measured before (left column) and during (right column) the biasing phase (No 108288). The dashed lines on top panels denote limiter locus. The vertical red lines in contour plots indicate the time when the two probes are at the same radial location ($r/a \approx 0.96$). (b) Frequency spectrum of V_n fluctuations detected by the fast probe at $r/a \approx 0.96$ before and during the biasing phase.

on the $k_\theta = k_{\theta 1} + k_{\theta 2}$ axis. One can see that the energy transfer to zonal flows ($k_\theta = 0$), shown by red positive values along the $k_{\theta 1} = -k_{\theta 2}$ line in the plot, arises mainly from smaller scales ($k_{\theta 1} \geq 1$). Note that k_θ here is normalized to the drift scale ρ_s . The results indicate a nonlocal energy cascading from drift-wave turbulence to zonal flows.

In addition, in the ISTTOK tokamak a coupling between the GAM-related LRC and local turbulent transport has been observed [19]. Plotted in figures 7(a) and (b) are the time evolution of the toroidal LRC (at $\tau = 0$) and local turbulence-driven particle flux $\Gamma_{E \times B} = \langle \tilde{n} \tilde{E}_\theta \rangle / B$ (\tilde{n} and \tilde{E}_θ being the density and poloidal electric field fluctuations, respectively). Both signals of the LRC and the flux are quite bursty. The

vertical dashed and solid lines show that the amplitudes of the LRC (related to GAM) and the turbulent flux vary inversely with time, i.e. when one is small the other is large, and vice versa. Such a coupling is further verified in figure 7(c), where the averaged flux decreases with increasing covariance (defined as cross-correlation without normalization) in V_n fluctuations [19]. This result implies a GAM modulation on local turbulent transport, in agreement with numerical calculations [25].

The common feature of the above biasing and spontaneous H-mode experiments is the development of edge mean E_r during the H-mode regime. Thus, the amplification of the LRC and zonal flows is closely linked to the development

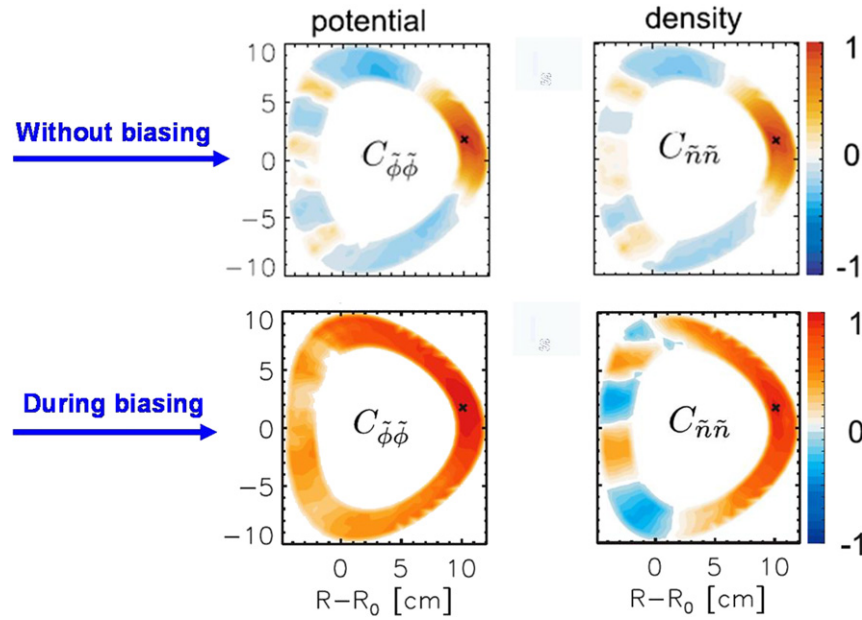


Figure 4. Increase in the LRC on both potential and density fluctuations during the biasing experiment in the TJ-K stellarator [18]. The cross-correlations are measured between the reference probe (x) and other poloidally separated probes at zero delay time.

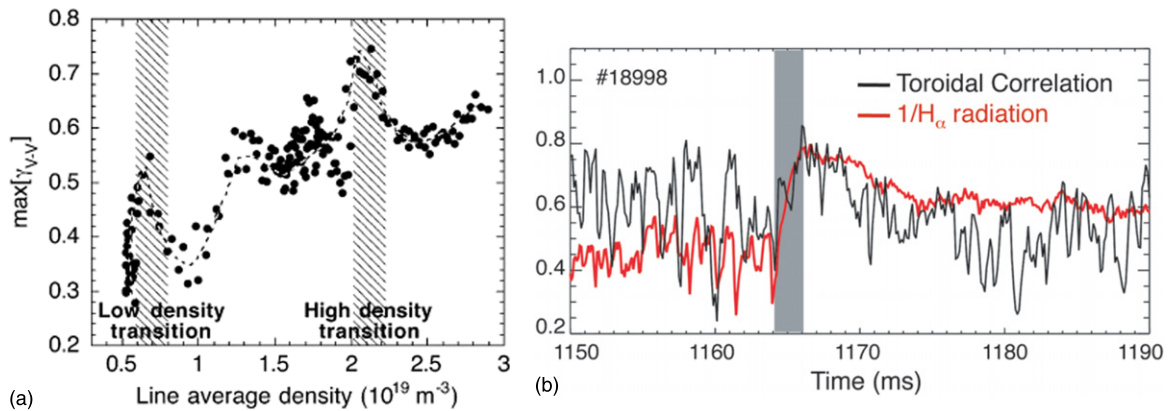


Figure 5. Increase in the LRC on V_{\parallel} fluctuations during a spontaneous L–H transition in the TJ-II stellarator [22]. (a) Maximum value of the LRC as a function of the line-averaged density in NBI plasmas, (b) time evolution of the maximum value of the LRC and the $1/H_{\alpha}$ signal. The shaded area in (b) indicates the L–H transition time.

of edge E_r and $E_r \times B$ sheared flows. The development of the LRC (zonal flows) driven by turbulence requires a mechanism for transferring the turbulent energy to large scales, such as Reynolds stress, e.g. via the eddy tilting mechanism. The impact of sheared flows on edge turbulent structures show results that are consistent with the picture of the shear stretching blobs as well as ordering, thus providing a possible explanation for the experimentally observed link between mean sheared flows and the development of LRCs [23, 26–28]. In addition, the zonal flow enstrophy and the enstrophy of drift-wave turbulence show a phase delay about $\pi/2$ [29, 30], which is an expected feature of a predator–prey oscillation [10–13]. The results are therefore in accordance with the theory of ‘zonal flows’ described by a predator–prey model, i.e. modes that are driven by zonal flow and turbulence interaction, and with a potential capability to regulate turbulent transport.

The LRCs have also been investigated in plasma regimes with reduced level of plasma fluctuations (H-mode). Experiments at the TJ-II stellarator [22] have shown that once

the transition to an improved confinement regime is completed, the level of the LRC gradually decreases, as can be seen in figure 5(b). Experiments in the ASDEX-Upgrade tokamak have shown that the LRC due to GAMs also strongly decrease in the H-mode regime [31]. Similar results have been observed in the JFT-2M tokamak [32].

3.2. Impact of RMP on the LRC

Comparative studies in tokamaks, stellarators and reversed field pinches have revealed significant differences in the properties of the LRC measured in the plasma edge. Whereas the LRCs are clearly observed in the plasma regions in tokamaks and stellarators with significant mean E_r and flow shear, no clear signature of the LRC was observed in the RFX-mod reversed field pinch experiments despite the highly sheared E_r observed [33]. The lack of LRCs in V_{\parallel} fluctuations in the RFX-mod may result from the high level of magnetic fluctuations observed in low-current RFP

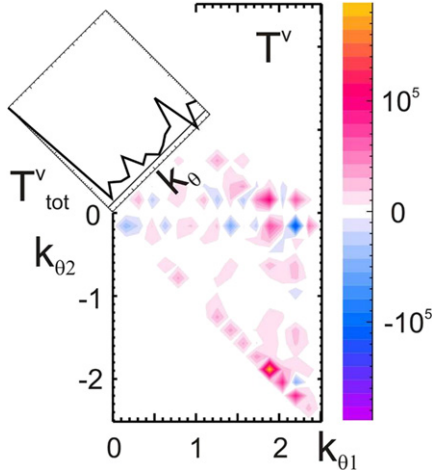


Figure 6. Nonlinear fluid kinetic energy transfer observed in the TJ-K stellarator [23].

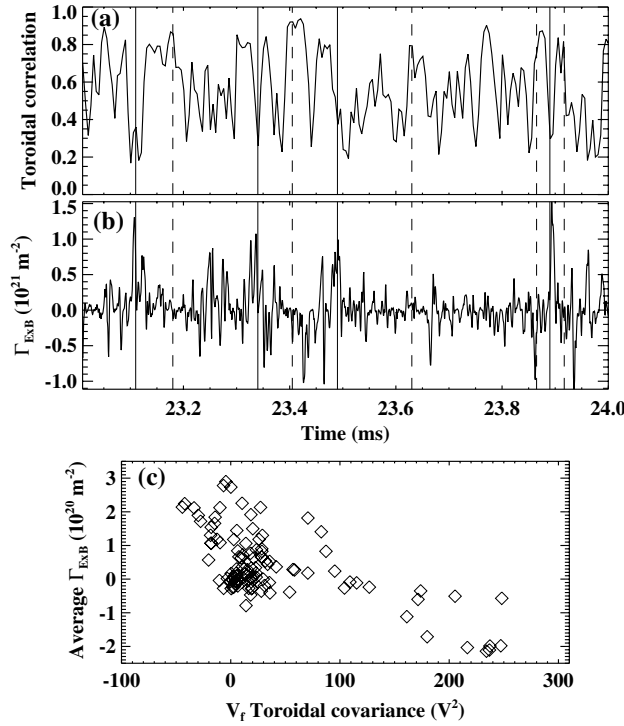


Figure 7. Time evolution of (a) the value of LRC ($\tau = 0$) on V_{\parallel} fluctuations and (b) fluctuation-induced particle flux. (c) Average particle flux against the V_{\parallel} covariance ($\tau = 0$) measured in the ISTTOK tokamak [19].

discharges: these discharges are characterized by the so-called multiple helicity state, where magnetic fluctuations induce a certain degree of stochasticity, as revealed by Poincaré plot reconstruction of the magnetic field lines [34]. Furthermore, the topology is complicated by the presence of $m = 0$ islands. These islands are found to modulate the plasma-wall interaction, field line connection length and also contribute to the formation of the radial electric field in the extreme periphery, modifying ion and electron diffusion processes and the resultant ambipolar electric field [20]. The series of islands modify the external region creating regions of high degree of stochasticity (X-point) and region of better confinement

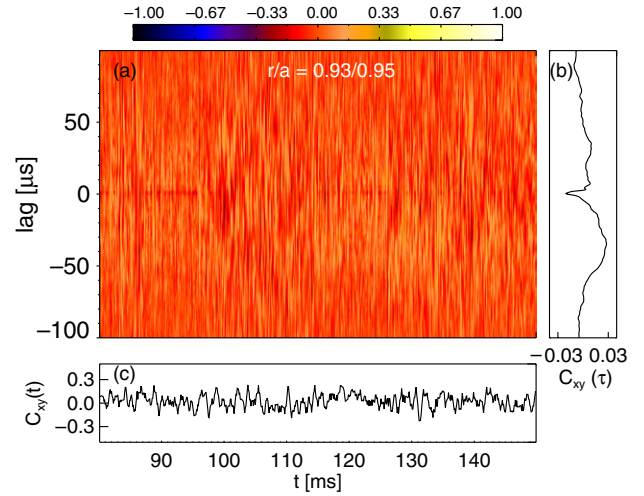


Figure 8. Absence of the LRC in the RFX-mod reversed field pinch. (a) Contour plot of the LRC between two floating potential tips (15 m away) as a function of time and time lag when the two probe tips are at about the same radial position ($r/a = 0.93$ and 0.95) in the plasma edge; (b) the averaged value of the LRC over the selected time interval and (c) time traces of the signed maximum of the absolute value of the LRC.

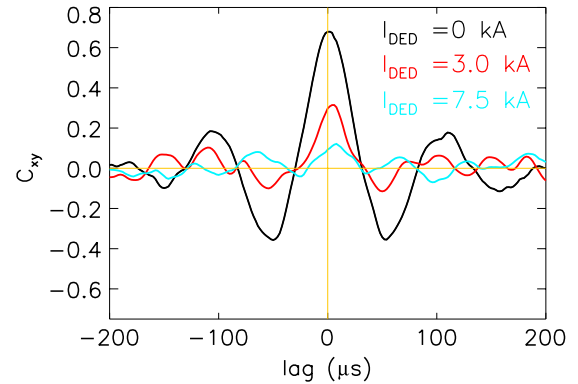


Figure 9. Maximum values of the LRC on V_{\parallel} fluctuations measured under different DED currents ($I_{\text{DED}} = 0, 3.0$ and 7.5 kA) in an $m/n = 6/2$ DED configuration at the edge ($r/a \approx 0.95$) of the TEXTOR tokamak (edge safety factor $q(a) = 5.0$).

(O-point) thus limiting the formation of zonal flow structures. In figure 8, an example of the LRC on V_{\parallel} fluctuations between two distant probes (at about the same radial position inside the LCFS) is shown as a function of time and time lag. The averaged value in the time interval chosen is shown in panel (b), from which it is clearly seen that the correlation is nearly zero (< 0.03). In the bottom panel the time evolution of the maximum of the absolute value of the LRC with the corresponding sign is shown, in order to emphasize that the maximum cross-correlation values do not exceed 0.25. Note that in the RFX-mod, at lower $q(a)$ values sporadic and bursty LRC are observed. But this is most likely due to reconnection events associated with a poloidally symmetric current sheet which propagates in the toroidal direction [35].

The above results are consistent with recent observations of the LRC in the RMP experiments at the TEXTOR tokamak. In TEXTOR the dynamic ergodic divertor (DED) system can ergodize the edge magnetic field lines and hence create a stochastic magnetic topology via the RMP with various base

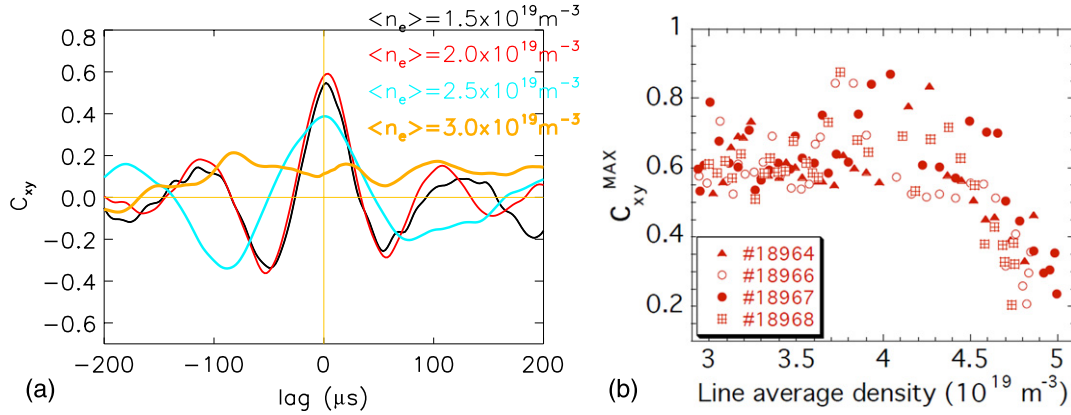


Figure 10. Reduction in the LRC with increasing plasma density towards density-limit in the TEXTOR tokamak and the TJ-II stellarator. (a) Maximum correlation value of the LRC on V_{\parallel} fluctuations measured in different density plasmas at the edge ($r/a \approx 0.95$) of TEXTOR [$q(a) = 5.9$]. (b) Maximum correlation value of the LRC on V_{\parallel} fluctuations as a function of plasma density in the TJ-II stellarator.

perturbation modes ($m/n = 12/4, 6/2$ and $3/1$). Details about the TEXTOR-DED system and related configurations can be found in [36]. With increasing DED current the ergodization on edge magnetic field lines is expected to be stronger. In figure 9 the maximum values of the long-range cross-correlation, C_{xy} , on V_{\parallel} fluctuations (when two probes are around the same radial location inside the LCFS, $r/a \approx 0.95$) are shown for three different DED currents ($I_{\text{DED}} = 0, 3.0$ and 7.5 kA) in an $m/n = 6/2$ DED configuration. The $I_{\text{DED}} = 0$ (black curve) corresponds to a standard ohmic discharge at TEXTOR, in which the GAM zonal flows are routinely observed inside the LCFS [37, 38]. The time lag on the cross-correlation function shows that the GAM oscillates at frequencies around $f = 10$ kHz (i.e. period $\approx 100 \mu s$). Note that here the ‘standard ohmic discharge’ differs from the ohmic discharge (before biasing) in the biasing experiment, where no GAM presents (see left column of figure 3) because of insertion of the biasing electrode into the LCFS, which alters the boundary conditions for GAM survival. From figure 9 one can clearly see that with increasing DED current the LRCs are gradually reduced. Similar results have also been seen in other DED configurations. As a consequence, these results reveal the impact of the RMP on the LRC and related zonal flows, and hence on plasma transport, as reported in [39].

For the influence of the RMP on the LRC and GAMs, two possible mechanisms are proposed. The first may be linked to parallel dynamics for the development of GAM zonal flows [40]. Without RMP, $k_{\parallel} \approx 0$ is subject to strong instabilities of modes, whereas with RMP these modes of GAMs are damped by resistivity because k_{\parallel} becomes finite due to nonzero radial components of magnetic field, B_r . The second mechanism is related to reduced E_r by the RMP. In the RMP experiments a typical feature observed is the reduction in edge mean E_r due to the parallel electron losses onto the wall along stochastic field lines [41, 42]. As stated earlier, the mean $E \times B$ sheared flows could tilt turbulence eddies and thus be helpful for the development of LRC. In contrast, the reduced edge mean E_r could decrease the zonal flow levels. Nevertheless, this paradigm cannot explain the absence of LRCs in the RFX-mod, where a highly sheared E_r is generally observed [33].

3.3. Impact of plasma density on the LRC in density-limit experiments

The LRC has also been investigated in the proximity of the density-limit in the TEXTOR tokamak and the TJ-II stellarator. Shown in figure 10(a) are the maximum values of the LRC on V_{\parallel} fluctuations detected in different density discharges at the edge ($r/a \approx 0.95$) of TEXTOR. In the figure $\langle n_e \rangle$ denotes the values of line-averaged density in several shots under the same edge safety factor of $q(a) = 5.9$. At low densities ($\langle n_e \rangle \leq 2 \times 10^{19} \text{ m}^{-3}$) the LRCs are quite large and vary only slightly with increasing density. However at higher densities ($\langle n_e \rangle > 2 \times 10^{19} \text{ m}^{-3}$) when approaching the density-limit, the LRC, which is also associated with GAM zonal flows, reduces rapidly with increasing plasma density. Similar results have also been observed in the TJ-II stellarator (see figure 10(b)), where the degree of the LRCs drops drastically with increasing density towards operational limits. In the density-limit discharges, the increase in plasma density usually induces a reduction in edge temperature and consequently a change in collisionality. In both machines, it is interesting to find that the reduction in the LRC due to increasing density is always accompanied by a reduction in edge mean radial electric field. Therefore, the results suggest the possible role of collisionality and the impact of mean $E \times B$ flow shear as well on the LRC and zonal flows.

4. Conclusions

A European transport project has been carried out among several fusion devices, including tokamaks, stellarators and a reversed field pinch, for investigating the possible link between the radial electric field, LRCs and edge bifurcations in fusion plasmas. In this paper the main results we reported are (i) the discovery of low-frequency LRCs in potential fluctuations that are amplified during the development of edge mean E_r using electrode biasing in the TJ-II/TJ-K stellarators and TEXTOR/ISTTOK tokamaks and during the spontaneous development of edge sheared flows in the TJ-II stellarator. Evidence of nonlocal energy transfer and GAM modulation on local turbulent flux has been observed in the TJ-K stellarator and ISTTOK tokamak, respectively. The results point to a

significant link between the $E \times B$ sheared flows, LRCs and transport bifurcations. (ii) Comparative studies in tokamaks, stellarators and reversed field pinches have revealed significant differences in the level of the LRC. The absence of the LRC in the RFX-mod reversed field pinch suggests a damping effect of magnetic perturbations on the LRCs, in agreement with observations in the RMP experiments in the TEXTOR tokamak. (iii) The degree of the LRCs is strongly reduced on approaching the plasma density-limit in the TEXTOR tokamak and the TJ-II stellarator, implying the possible role of collisionality or/and the impact of mean $E_r \times B$ flow shear on zonal flows.

Euratom © 2011.

References

- [1] Wagner F. *et al* 1982 *Phys. Rev. Lett.* **49** 1408
- [2] Itoh S. *et al* 1988 *Phys. Rev. Lett.* **60** 2276
- [3] Groebner R. *et al* 1990 *Phys. Rev. Lett.* **64** 3015
- [4] Ida K. *et al* 1990 *Phys. Rev. Lett.* **65** 1364
- [5] Biglary H. *et al* 1990 *Phys. Fluids B* **2** 1
- [6] Fujisawa A. *et al* 2004 *Phys. Rev. Lett.* **93** 165002
- [7] Gupta D.K. *et al* 2006 *Phys. Rev. Lett.* **97** 125002
- [8] Xu G.S. *et al* 2003 *Phys. Rev. Lett.* **91** 125001
- [9] Liu A.D. *et al* 2009 *Phys. Rev. Lett.* **103** 095002
- [10] Diamond P.H. *et al* 2005 *Plasma Phys. Control. Fusion* **47** R35
- [11] Fujisawa A. *et al* 2009 *Nucl. Fusion* **49** 013001
- [12] Diamond P.H. *et al* 1994 *Phys. Rev. Lett.* **72** 2565
- [13] Kim E.J. and Diamond P.H. 2003 *Phys. Plasmas* **10** 1698
- [14] Fujisawa A. *et al* 2006 *Plasma Phys. Control. Fusion* **48** A365
- [15] Xia H. *et al* 2006 *Phys. Rev. Lett.* **97** 255003
- [16] Pedrosa M.A. *et al* 2008 *Phys. Rev. Lett.* **100** 215003
- [17] Xu Y. *et al* 2009 *Phys. Plasmas* **16** 110704
- [18] Manz P. *et al* 2009 *Phys. Plasmas* **16** 042309
- [19] Silva C. *et al* 2008 *Phys. Plasmas* **15** 120703
- [20] Scarin P. *et al* 2011 Topology and transport in the edge region of RFX-mod helical regimes *Nucl. Fusion* submitted
- [21] Silva C. *et al* 2009 Experimental evidence of coupling between local transport and large scale fluctuations in ISTTOK 2nd EFDA TTG Workshop (Culham, UK, 16–18 September 2009)
- [22] Hidalgo C. *et al* 2009 *Europhys. Lett.* **87** 55002
- [23] Manz P. *et al* 2009 *Phys. Rev. Lett.* **103** 165004
- [24] Camargo S.J. *et al* 1995 *Phys. Plasmas* **2** 48
- [25] Ramisch M. *et al* 2003 *New J. Phys.* **5** 12
- [26] Alonso A. *et al* 2006 *Plasma Phys. Control. Fusion* **48** B465
- [27] Alonso A. *et al* 2009 *Europhys. Lett.* **85** 25002
- [28] Ramisch M. *et al* 2010 *Plasma Phys. Control. Fusion* **52** 124015
- [29] Manz P., Ramisch M. and Stroth U. 2010 *Phys. Rev. E* **82** 056403
- [30] Estrada T. *et al* 2010 *Europhys. Lett.* **92** 35001
- [31] Conway G. *et al* 2010 *Proc. 23rd Int. Conf. on Fusion Energy 2010 (Daejeon, South Korea 2010)* (Vienna: IAEA) CD-ROM file EXC/7-1 and <http://www-naweb.iaea.org/napc/physics/FEC/FEC2010/html/index.htm>
- [32] Ido T. *et al* 2006 *Nucl. Fusion* **46** 512
- [33] Vianello N. *et al* 2005 *Phys. Rev. Lett.* **94** 135001
- [34] Vianello N. *et al* 2009 *Nucl. Fusion* **49** 045008
- [35] Zuin M. *et al* 2009 *Plasma Phys. Control. Fusion* **51** 035012
- [36] Finken K.H. *et al* 2004 *Plasma Phys. Control. Fusion* **46** B143
- [37] Shesterikov I. *et al* 2010 Investigation of GAM zonal flows in the TEXTOR tokamak *Proc. 37th EPS Conf. on Plasma Physics (Dublin, Ireland, 2010)* P1.1090
- [38] Xu Y. *et al* Influence of resonant magnetic perturbation (RMP) and plasma density on the long-range correlation and GAM zonal flows at TEXTOR 3rd EFAD TTG Meeting and 15th EU-US TTF Workshop (Cordoba, Spain, 2010) O4.07 and <http://www-fusion.ciemat.es/ttg2010/>
- [39] Xu Y. *et al* 2006 *Phys. Rev. Lett.* **97** 165003
- [40] Reiser D. 2010 private communication, Institute of Energy and Climate Research—Plasma Physics, Forschungszentrum Jülich, Germany
- [41] Yang X.Z. *et al* 1991 *Phys. Fluids B* **3** 3448
- [42] Xu Y. *et al* 2007 *Nucl. Fusion* **47** 1696